Journal of King Saud University – Science (2014) 26, 311–322

King Saud University
Journal of King Saud University – Science
www.ksu.edu.sa
www.sciencedirect.com

ORIGINAL ARTICLE

Comparative assessment of rheological properties of gelatin or gellan in maize starch – egg white composite gels

Thuan-Chew Tan [a,*], Wan-Teck Foo [a], Min-Tze Liong [b], Azhar Mat Easa [a]

[a] Food Technology Division, School of Industrial Technology, Universiti Sains Malaysia, 11800 Minden, Penang, Malaysia
[b] Bioprocess Technology Division, School of Industrial Technology, Universiti Sains Malaysia, 11800 Minden, Penang, Malaysia

Received 18 July 2013; accepted 5 February 2014
Available online 15 February 2014

KEYWORDS
Composite gels;
Component gels;
Gellan;
Gelatin;
Rheological characteristics

Abstract Single component gels (SCG) were formed from gelatin, gellan, maize starch or egg white, while binary component gels (BCG) and tertiary component gels (TCG) were formed by mixing gelatin or gellan with maize starch or/and egg white. All gels were evaluated by stress relaxation and uniaxial compression tests. Each type of SCG exhibited distinct rheological characteristics. The effects of gelatin or gellan proportions on the rheological properties of BCG and TCG were investigated using mixture design experiments. Gelatin and gellan yielded composite gels that were remarkably different in terms of rheological behaviors. All BCG and TCG blends showed antagonistic effects; the composite gels were weaker and more brittle as compared to the SCG. Gellan composite gels were comparatively weaker and possessed more viscous behavior compared to those of gelatin-based due to different gelling mechanisms, in which the latter had yielded denser network structures as compared to the former.
© 2014 King Saud University. Production and hosting by Elsevier B.V. All rights reserved.

1. Introduction

Rheology is the science of deformation and flow of a matter under controlled conditions and it helps to understand how food structure responds to the applied force and deformation. Rheological measurements are useful in quantifying the mechanical behavior of food structure. Hence, it has been used to complement the information on gel network structure and interactions among the components of the system. Furthermore, rheological information of a food gel can give an indication of some of the sensory and textural characteristics (Burey et al., 2009). In general, the rheological properties of food systems can be evaluated with two kinds of tests: small deformation–stress relaxation and large deformation–fracture properties' tests.

Stress relaxation test is commonly used to quantify viscoelastic properties of gels that are related to crosslinks within the networks by monitoring stress changes with time for a short or long period of time. In general, stress relaxation demonstrates the transient mechanical behavior of gels through the

* Corresponding author. Tel.: +60 4 6535207; fax: +60 4 6573678.
E-mail address: thuanchew@usm.my (T.-C. Tan).
Peer review under responsibility of King Saud University.

Production and hosting by Elsevier

1018-3647 © 2014 King Saud University. Production and hosting by Elsevier B.V. All rights reserved.
http://dx.doi.org/10.1016/j.jksus.2014.02.001

relative ability of the gel network to withstand the targeted strain. The gel structure could be revealed through the amount of energy that the network absorbed or dissipated. For stress relaxation tests, fracture does not occur and the energy intake during compression is not completely stored in the material but is partly dissipated. Upon relaxation, a covalently cross-linked network that is also considered as an ideal gel would show no stress relaxation (Shim and Mulvaney, 2001). On the contrary, the energy stored in viscoelastic gels is substantially dissipated through several ways such as release of compression-induced hydraulic pressure, entanglement coupling of chains in covalent networks, shifting of crosslinks in non-covalent networks (Tang et al., 1998), or friction between dispersed particles and network frames during the viscous flow through the network (Luyten and van Vliet, 1995).

The stress and strain at fracture point are known as fracture stress and fracture strain. Fracture stress may be interpreted as the strength of a gel, while fracture strain is a measure of the deformability. The gel strength and deformability depend on the number and the type of bonds within the gel network (Mao and Tang, 1999; Renkema, 2004; Weijers et al., 2006). Parts of the gel structural elements were damaged during deformation; however, the gel would only rupture when the deformation achieved sufficient strain where the structural damage reached a certain microscopic scale (van Vliet, 1996; Zhang, 2004). Generally, fracture strain for a gel system is independent on biopolymer concentrations but is closely related to the type of molecule forming the gel network (Zhang, 2004). Gels compose of relatively thin network strands and small homogeneous pores would fracture at low strain values, while gels that fracture at high strain values are composed of thicker strands and relatively larger homogeneous pores (Weijers et al., 2006).

Gellan has been proposed as one of the gelatin alternatives in food applications (Morrison et al., 1999). It was hypothesized that gellan would reveal the same gelling effects as gelatin in composite gel systems, as gelatin and gellan are both helix-forming biopolymers that form gels on cooling. However, gelatin gels are soft, elastic, translucent and thermoreversible (Glicksman, 1969; Ledward, 2000), while low-acyl Gll gels are clear, firm to touch, brittle and usually non-thermoreversible (Huang et al., 2007; Williams and Philips, 2003). The strength and texture of gellan gels are dependent on ionic strength, while those of gelatin gels depend more on the concentration of gelatin (Lee et al., 2003; Morris et al., 2012; Panouillé and Larreta-Garde, 2009; Pérez-Campos et al., 2012).

It was hypothesized that by manipulating the proportions of gelatin or gellan with maize starch and egg white, we could yield composite gels with similar rheological properties. To our knowledge, very little studies have been performed on comparative assessment of composite gels prepared from gelatin and gellan. Therefore, composite gels composed of maize starch and/or egg white were selected as model systems in this study to investigate the feasibility of gellan as a gelatin replacer by characterizing and comparing these two systems. The objective of this study was to comparatively study the influence of ingredient composition on the rheological properties (small deformation-stress relaxation and large deformation-fracture properties) of gelatin and gellan in composite gel systems containing maize starch or/and egg white.

2. Materials and methods

2.1. Materials

Gelatin (source: bovine, bloom strength 160, pH 5.3) was obtained from Halagel Sdn Bhd, Kedah, Malaysia. Low-acyl gellan was supplied by Fluka Chemical Corp., Ronkonkoma, USA. Maize starch was purchased from Roquette Freres S. A., Lestrem, France. Egg albumen powder (instant high gel, EAP-HG) was purchased from Belovo S. A., Bastogne, Belgium. This high-gelling egg albumen powder contains protein and moisture contents of 82.5% and 5.9%, respectively.

2.2. Gel preparation

The four selected biopolymers employed in this section were of common ingredients used for a gelling purpose in food products, namely maize starch (MS), egg white (EW), gelatin (Glt) and gellan (Gll). Single component gels (SCG) were formed from Glt, Gll, MS or EW, while binary component gels (BCG) and tertiary component gels (TCG) were formed by mixing Glt or Gll with MS or/and EW powders. SCG with specific targeted modulus values (24,000 N m^{-2}) were used as a benchmark against composite gels to yield free-standing gels (Foo et al., 2013). During preliminary work, MS and EW required 13% (w/w) and 9% (w/w) of biopolymers, respectively to yield SCG with modulus values of in close proximity to 24,000 N m^{-2}. However, the modulus values for Glt and Gll deviated from the targeted modulus as the concentrations of biopolymers were adjusted in order to prepare gels that suited the whole experimental conditions, where free-standing gels were necessary for the analyses. For Glt-SCG, the amount of biopolymer selected was 11% (w/w) although the modulus obtained (~19,000 N m^{-2}) was lower than the targeted value. However, it was not suitable to raise the amount of Glt for composite gel formulations due to the effect of limited water for a complete biopolymer hydration. As for Gll-SCG, the selected amount of biopolymer (2.5%, w/w), yielded SCG with modulus (~35,000 N m^{-2}) that exceeded the target values. However, it was not suitable to prepare Gll-SCG with the targeted modulus value (24,000 N m^{-2}) since below 2.5% (w/w) of Gll concentration no free-standing composite gels (Gll-BCG and Gll-TCG) could be formed. Thus, the concentrations of MS, EW, Glt and Gll were 13%, 9%, 11% and 2.5% (w/w), respectively.

The stock biopolymer (Glt, Gll, MS and EW) dispersions were prepared separately. The individual biopolymers were dispersed in distilled water and were then left overnight at 15 °C (Sanyo Electric Co. Ltd., MIR-254, Moriguchi, Japan) to ensure complete swelling. Glt and Gll dispersions were dissolved by heating the dispersions at 80 °C in a water bath (Memmert GmbH & Co. KG, WB22, Schwabach, Germany) and stirred constantly until clear solutions were formed. MS slurry and EW solution were vacuum-degassed using diaphragm vacuum pump (Vacuubrand GmbH & Co. KG, ME 2C, Wertheim, Germany) for 20 min under continuous stirring on a magnetic stirrer (Heidolph Instruments GmbH & Co. KG, MR Hei-Tec, Schwabach, Germany) to avoid bubble formation. All the biopolymer stock solutions were kept at 50 °C in a water bath prior to blend preparation as depicted in Table 1.

Table 1 Combinations of composite gels formulated with maize starch (MS), egg white (EW) and gelatin (Glt) or gellan (Gll) in the augmented simplex centroid design.

Run	Component proportions[a]					
	A: MS	B: EW	C: Glt	A: MS	B: EW	C: Gll
1	0.50	0.00	0.50	1.00	0.00	0.00
2	1.00	0.00	0.00	0.42	0.42	0.17
3	0.50	0.50	0.00	0.00	0.50	0.50
4	1.00	0.00	0.00	0.17	0.42	0.42
5	0.67	0.00	0.33	0.00	0.67	0.33
6	0.17	0.42	0.42	0.50	0.50	0.00
7	0.00	0.67	0.33	0.42	0.17	0.42
8	0.33	0.00	0.67	1.00	0.00	0.00
9	0.42	0.17	0.42	0.67	0.00	0.33
10	0.67	0.17	0.17	0.33	0.67	0.00
11	0.00	0.33	0.67	0.00	0.00	1.00
12	0.33	0.67	0.00	0.17	0.17	0.67
13	0.33	0.33	0.33	0.50	0.00	0.50
14	0.42	0.42	0.17	0.17	0.67	0.17
15	0.17	0.67	0.17	0.00	1.00	0.00
16	0.00	0.00	1.00	0.33	0.33	0.33
17	0.67	0.33	0.00	0.00	1.00	0.00
18	0.17	0.17	0.67	0.67	0.17	0.17
19	0.00	0.00	1.00	0.00	0.33	0.67
20	0.00	0.50	0.50	0.00	0.00	1.00
21	0.00	1.00	0.00	0.67	0.33	0.00
22	0.00	1.00	0.00	0.33	0.00	0.67

[a] A + B + C = 1 or 100%.

Gels were prepared according to the method as described by Foo et al. (2013) with slight modifications. The designated blends were transferred into syringes (volume: 20 mL; inner diameter: 19 mm) and heated at 95 °C for 20 min. A thin layer of paraffin oil was dropped on the surface of the samples in each syringe to prevent excessive water evaporation. All the samples were cooled to room temperature (25 °C) and subsequently refrigerated at 4 °C for at least 18 h. The gels were unmolded and cut into 20 mm in length and were left to equilibrate at 15 °C for at least 1 h prior to analysis.

2.3. Design of experiment

Design Expert (Stat-Ease Co., Minneapolis, USA) was used to prepare an experimental design and samples were prepared according to an augmented simplex-centroid mixture design with 10 candidate points. In addition, 9 experimental candidate points were added to verify the absence for lack of fit and 3 candidate points were introduced as replicates. Thus, an experimental design with 22 candidate points was obtained (Table 1).

The experimental domains consisted of different proportions of components of *A* (MS), *B* (EW) and *C* (Glt or Gll). The proportional levels of these gelling components were set in between 0% and 100% (w/w); ($A + B + C = 100$). The experimental domain was within a regular triangle. The vertices of the simplex represented the pure components, while the edges of the triangle represented the two-component blends. The centroid of the triangle corresponds to the mixture with equal proportions (1/3: 1/3: 1/3) from each of the components and points within the triangle represented the three-component blends.

2.4. Stress relaxation test

Small deformation properties of gels were determined in transient mode through stress relaxation measurements. Stress relaxation tests were conducted using a TA-TX2 Texture Analyzer (Stable Micro Systems Ltd., Surrey, UK), attached with a 15 kg load cell. The method applied was according to Kampf and Nussinovitch (1997) with modification on setting to suit the experimental conditions. A gel sample was compressed at pre-test speed of 1 mm s^{-1} and test speed of 0.5 mm s^{-1} to 20% of strain and the gel was subsequently allowed to relax for 60 s (Hongsprabhas, 2011). Three measurements were recorded for each type of gel.

The obtained relaxation curves were normalized (Eq. (1)) and linearized (Eq. (2)) according to the two-step method by Peleg and Normand (1983) as shown in the following equations:

$$Y_t = (F_0 - F_t)/F_0 \tag{1}$$

$$t/Y_t = k_1 + k_2 t \tag{2}$$

where, Y_t is the decaying parameter; F_0 and F_t are the initial force and the momentary force at time t, respectively, while k_1 (s) and k_2 (dimensionless) are constants. The reciprocal of k_1 is the initial rate of relaxation and can be interpreted as the viscous component. For food materials, k_2 is a better representative of elastic nature and not of solid nature (Singh et al., 2006).

2.5. Uniaxial compression test

The rheological behaviors of gels were determined through uniaxial compression tests by using a TA-TX2 Texture Analyzer, attached with a 30 kg load cell. A 75 mm diameter compression platen was used to compress a cylindrical sample at a constant speed of 1 mm s^{-1} until fracture. The bottom plate and the top of the gel were covered with a thin layer of paraffin oil to allow sample expansion in order to avoid the barrel effect during compression. At least five measurements were recorded for each type of gel. The obtained force–time data were then converted into true (Hencky's) stress–strain curves using following equations:

$$\text{True (Hencky's) stress } \sigma_{\text{true}} = F_t/A_0 \times H_t/H_0 \tag{3}$$

$$\text{True (Hencky's) strain } \varepsilon_{\text{true}} = \ln((H_0 - H_t)/H_0) \tag{4}$$

where, F_t is the force after deformation time of t, A_0 is the sample cross-sectional area before deformation (for cylindrical gels, $A_0 = \pi R_0^2$), R_0 and H_0 are the initial radius and height of the samples, respectively; while R_t and H_t are the sample radius and height after deformation of t (Wium and Qvist, 1997).

2.6. Mixture regression and statistical analysis

Scheffe's canonical equations for three components were fitted to data collected at each experimental point using multiple regression analysis. Mixture regression analysis was performed by Design Expert software to compute predictive models for each tested response. The data were initially fitted to all available mixture regression models of increasing complexity, from linear to full quadratic. The adequacy of model fitness was

judged based on model significance, significance of lack-of-fit and determination coefficient (adjusted R^2). The adjusted R^2 describes the proportion of variation in the responses that is explained by the model and the value has been adjusted for the number of terms in the model. The best fitted model was then determined based on the insignificant of lack-of-fit and the highest adjusted R^2 with Scheffe's canonical models. Variables in the regression model were referred to as estimated coefficients. The effect of linear, binary and ternary terms was then justified based on estimated coefficients of the model equation for each parameter. The estimated coefficients were computed in actual components, which were represented by the weight percentage of different components (Ibrahim et al., 2010).

The statistical evaluations were performed using SPSS 14.0 for Windows software. For each parameter studied, the significant difference was determined through One-way analysis of variance (ANOVA) at the level of $P < 0.05$. Duncan's multiple range test was applied to compare significant differences among mean values.

3. Results and discussion

Three main categories of gels were defined, i.e., single component gel (SCG), binary composite gel (BCG) and ternary composite gel (TCG). SCG composed of a single type of biopolymer. BCG and TCG consisted of two and three types of biopolymers, respectively. The BCG and TCG were prepared according to the blend ratios that were generated by the Design Expert software for the mixture design experiment. The rheological properties of the gels were characterized through small and large deformations.

3.1. Small deformation-stress relaxation

In this study, all the gels were not physically stable thus it is not suitable to conduct long term determinations of stress relaxation. Therefore, the relaxation parameters were determined for a short duration and Peleg's mathematical model was applied to characterize the relaxation behaviors of the gels. Two parameters were derived from the equation of Peleg's model, i.e., k_1 and k_2. The value of k_1 is the intercept of a linearized relaxation curve, and the reciprocal of k_1 represents the initial decay rate. For a pure liquid material, k_1 is equal to zero, while an ideal elastic material shows k_1 approaching infinity. The rate of relaxation would depend on pore size, capillary forces, viscous flow and particle interactions (Houzè et al., 2005). On the other hand, k_2 could be more indicative of the general rheological characteristics of gels since it could represent the degree of solidity, i.e., it is indirectly related to the volume of pores present per unit area. The higher the k_2 value, the higher the solid per unit area (Jaya and Durance, 2008). Peleg and Normand (1983) reported that solid foods (e.g., corn kernels) exhibited high k_2 values, while soft or semi-solid foods (e.g., cheese) showed values closed to unity, which also represented viscous properties.

3.1.1. Stress relaxation behavior of SCG

Four groups of SCG were prepared namely [Glt-SCG], [Gll-SCG], [MS-SCG] and [EW-SCG]. For all SCG, the force increased steeply and linearly during compression until the targeted 20% strain level (Fig. 1a). Glt-SCG and MS-SCG showed only slight relaxation responses and the decay in force was not obvious. Contrarily, the relaxation curves for Gll-SCG and EW-SCG illustrated a sharp decay during the initial phase of relaxation (~10 s). Subsequently, the force decayed gradually to approach the residual force values. The relaxation curves of SCG were fitted by Peleg's equation and the relaxation parameters are presented in Table 2.

The value of F_{max} represents the initial firmness of the gel at 20% of compression strain. The k_1 value reflects the strength and flexibility of the gel network, while k_2 value indicates the degree of solidity or the density of the gel structure (Jaya and Durance, 2008). Generally, gels with higher k_1 value (slower relaxation) are composed of stronger and more flexible strands.

Glt-SCG exhibited the lowest level of F_{max} and this could be attributed to the flexible network strands that were able to distribute force during compression (Table 2). The k_1 value of Glt-SCG was outrageously higher (~220 s) compared to the other SCG (k_1 ranged between 14 and 60 s). This could be explained by the strong and elastic network strands of Glt-SCG absorbed most of the energy during compression and were subsequently stored in the strands. In addition, Glt-SCG showed a relatively high level of k_2 (~16) implying that the gel structure was compact and there was no perceptible viscous component.

Gll-SCG showed the highest level of F_{max} among all the SCG (Table 2). The high level of firmness in Gll-SCG might owe to the brittle and rigid network strand. Despite, the water content in Gll-SCG was very high and thus the built-up hydraulic pressure during compression could also contribute to the initial firmness. However, Gll-SCG had little capability of storing energy as the stress was dissipated rapidly and substantially as indicated by the lowest k_1 value and the highest amount of force decayed (Fig. 1a). Gll-SCG consisted of ~97% water in supporting the gel matrix and water was held within the void space via capillary forces. The major factor responsible for stress relaxation in Gll-SCG was due to the release of hydraulic pressure (Tang et al., 1998). Moreover, the lowest value of k_2 implied that the gel structure of Gll-SCG was loose and consisted of a large part of viscous components.

MS-SCG and EW-SCG displayed similar F_{max}, however, the k_1 value of MS-SCG was relatively higher than EW-SCG (Table 2). This suggests that the network of MS-SCG was relatively stronger, more flexible and thus able to store higher level of energy (lower amount of dissipated energy) than EW-SCG. The value of k_2 of MS-SCG was the highest among all other SCG implying that the network structure of MS-SCG was the most solid and compact. This might due to the highest amount of biopolymer used to form the gel. On the contrary, EW-SCG exhibited relaxation response owed to the dissipated stress via internal rearrangement of protein aggregates (Shim and Mulvaney, 2001). The k_1 value of EW-SCG was of approximately onefold lower than MS-SCG, which could be attributed to the rigid and less deformable network of EW (Table 2). Besides, EW-SCG displayed significant viscous characteristic as indicated by the low level of k_2.

3.1.2. Stress relaxation behavior of BCG

Five groups of BCG were prepared namely [MS:EW], [MS:Glt], [MS:Gll], [EW:Glt] and [EW:Gll]. The stress

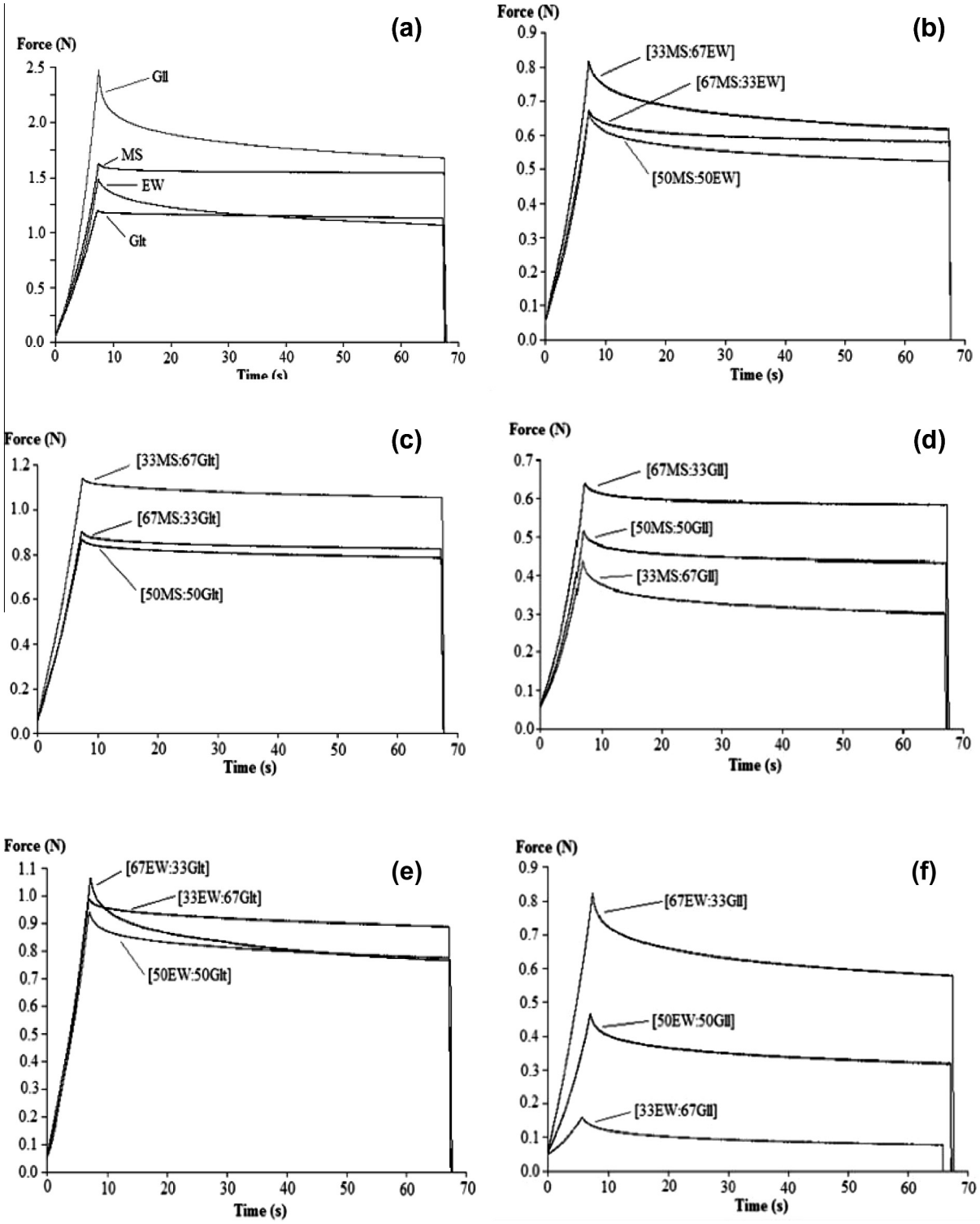

Figure 1 Stress relaxation curves of (a) SCG and BCG: (b) [MS:EW], (c) [MS:Glt], (d) [MS:Gll], (e) [EW:Glt] and (f) [EW:Gll].

relaxation curves of BCG are displayed in Fig. 1b–f. Generally, the combinations as well as the proportions of gel components resulted in different relaxation behaviors of BCG where the force decayed slowly with time. This trend is similar to that reported by Joshi et al. (2014) where stress values of lentil starch-lentil protein composite gels decreased with time and tended to attain a finite equilibrium stress value. According to Hibberd and Wallace (1966), this behavior of gel is attributed to the destruction of weak bonds while the strong bonds remain unaffected by a mechanical deformation.

All [MS:EW]-BCG exhibited relaxation, however, the relaxation behavior of BCG formed at the higher ratio of MS became less noticeable (Fig. 1b). The relaxation responses of [MS:Glt]-BCG were negligible and similar to both of the

Table 2 Stress relaxation parameters[a] of single component gel.

SCG[b]	F_{max} (N)	k_1 (s)	k_2 (−)
Glt (11%, w/w)	1.19 ± 0.03^{C}	218.47 ± 14.06^{A}	16.06 ± 1.40^{A}
Gll (2.5%, w/w)	2.43 ± 0.40^{A}	13.82 ± 0.23^{D}	2.93 ± 0.03^{C}
MS (13%, w/w)	1.59 ± 0.05^{B}	58.46 ± 7.71^{B}	18.90 ± 1.66^{A}
EW (9%, w/w)	1.50 ± 0.04^{B}	27.55 ± 0.85^{C}	3.16 ± 0.05^{B}

[a] Data are mean ± standard deviation of 5 replicates. Values with different upper superscript letters (A–D) within a column are significantly ($P < 0.05$) different between samples.
[b] SCG = single component gel, MS = maize starch, EW = egg white, Glt = gelatin, Gll = gellan.

MS-SCG and Glt-SCG, which were highly elastic and dissipated minimal amount of stress during relaxation (Fig. 1c). As for [MS:Gll]-BCG, the extent of relaxation increased with the increasing proportions of Gll (Fig. 1d). The relaxation behaviors of both [67EW:33Glt]-BCG and [67EW:33Gll]-BCG were similar (Fig. 1e and f). However, the relaxation responses deviated with the increasing ratio of Glt or Gll in the EW-BCG. For [EW:Glt]-BCG, the relaxation responses were less pronounced with the increasing proportions of Glt. As for [EW:Gll]-BCG, the magnitudes of the initial firmness decreased remarkably with the increase of Gll proportions.

The effects of component proportions on stress relaxation parameters for all the BCG are illustrated in Fig. 2. The F_{max} values of all [MS:EW]-BCG were reduced to approximately half as compared to the respective SCG (Fig. 2a and Table 2). The F_{max} value of [33MS:67EW]-BCG was significantly ($P < 0.05$) higher than other [MS:EW]-BCG, although the solidity of the gel was the lowest (lowest k_2) (Fig. 2a (i) and c (i)). The high level of firmness might be attributed to the strong network strands within the gel structure as shown by the low k_1 value (Fig. 2b (i)). As the proportions of EW increased, the initial firmness of [MS:EW]-BCG increased while the network structure became less compact as illustrated by the significant ($P < 0.05$) decline in k_2 values. This reveals that EW might be the predominant component contributed to the network structure, whereas MS contributed to the solidity of the gels.

The F_{max} of [33MS:67Glt]-BCG was significantly ($P < 0.05$) higher than other [MS:Glt]-BCG and was almost similar to the Glt-SCG (Fig. 2a (ii) and Table 2). From the values of k_1, it could be observed that the networks of [MS:Glt]-BCG became more flexible and stronger as the proportions of Glt increased (Fig. 2b (ii)). However, the value of k_2 of [MS:Glt]-BCG with equal proportions of MS and Glt was significantly ($P < 0.05$) lower indicating that the gel structure was less compact (Fig. 2c (ii)).

The F_{max} values of all [MS:Gll]-BCG were relatively lower as compared to their respective SCG (Fig. 2a (iii)). For [MS:Gll]-BCG, both the k_1 and k_2 values decreased significantly ($P < 0.05$) with increasing proportions of Gll (Fig. 2b (iii) and c (iii)). This demonstrates that the network strands of [MS:Gll]-BCG were less elastic and the gel structures became less compact, therefore more energy was dissipated during relaxation.

The F_{max} values of [EW:Glt]-BCG were in a narrow range revealing the proportions of EW and Glt did not affect the initial firmness of the gels (Fig. 2a (iv)). However, the values of k_1 and k_2 increased significantly ($P < 0.05$) with the increasing proportions of Glt (Fig. 2b (iv) and c (iv)). As Glt proportions increased, the network strands of [EW:Glt]-BCG became stronger and more elastic, furthermore the gel structure became more compact. This implies that Glt strands contributed predominantly to the structural properties of the gels.

The magnitudes for all the stress relaxation parameters (i.e., F_{max}, k_1 and k_2) decreased significantly ($P < 0.05$) with the increasing proportions of Gll in [EW:Gll]-BCG (Fig. 2a (v) c (v)). Although the initial firmness for Gll-SCG was the highest among all the SCG, the [EW:Gll]-BCG became less firm with the increasing proportions of Gll. The increased content of Gll yielded BCG with less compact gel structure with more rigid and brittle network strands. Furthermore, the [EW:Gll]-BCG with higher Gll proportion consisted more viscous components and therefore the gel networks were not able to store the built-up energy during compression.

3.1.3. Stress relaxation behavior of TCG

The purpose of using mixture design experiment in this section was to reveal the influence of component proportions on the linear deformation of composite gels. Thus, the statistical analysis was only discussed briefly. The behavior tendencies of stress relaxation responses for both Glt-TCG and Gll-TCG were described based on the corresponding contour and surface plots (Fig. 3a–c). All the F_{max}, k_1 and k_2 responses for both the Glt-TCG and Gll-TCG systems were fitted adequately by cubic model except for k_1 response for Glt-TCG, which was fitted by quadratic model. For both Glt-TCG and Gll-TCG, the regression coefficients indicated that all the binary combinations had antagonistic effects on F_{max}, k_1 and k_2. These effects could be also observed in the pattern of the respective contour and surface plots.

Generally, the F_{max} values of Glt-TCG increased with the increasing proportions of MS; however, the increasing Glt proportions resulted in higher level of F_{max} for Glt-TCG with equal proportions of MS and EW (Fig. 3a (i)). Besides, the k_1 value of Glt-TCG increased with the increasing Glt proportions indicating that most energy was stored and only a small amount of energy was dissipated attributed to their strong and elastic network strands (Fig. 3b (i)). This finding was in line with the results in Section 3.1.1 where the k_1 value of Glt-SCG was the highest among the examined SCG. This suggests that Glt was the main component contributed to the elastic characteristic in these TCG systems. The gel structure of Glt-TCG became less compact with the increasing proportions of EW as represented by the decrease in k_2 values (Fig. 3c (i)), suggesting that EW was the main component that reduced the degree of solidity of the Glt-TCG. Low level of k_2 in the presence of high level of EW was predictable since EW-SCG scored the lowest k_2 value, as reported in Section 3.1.1.

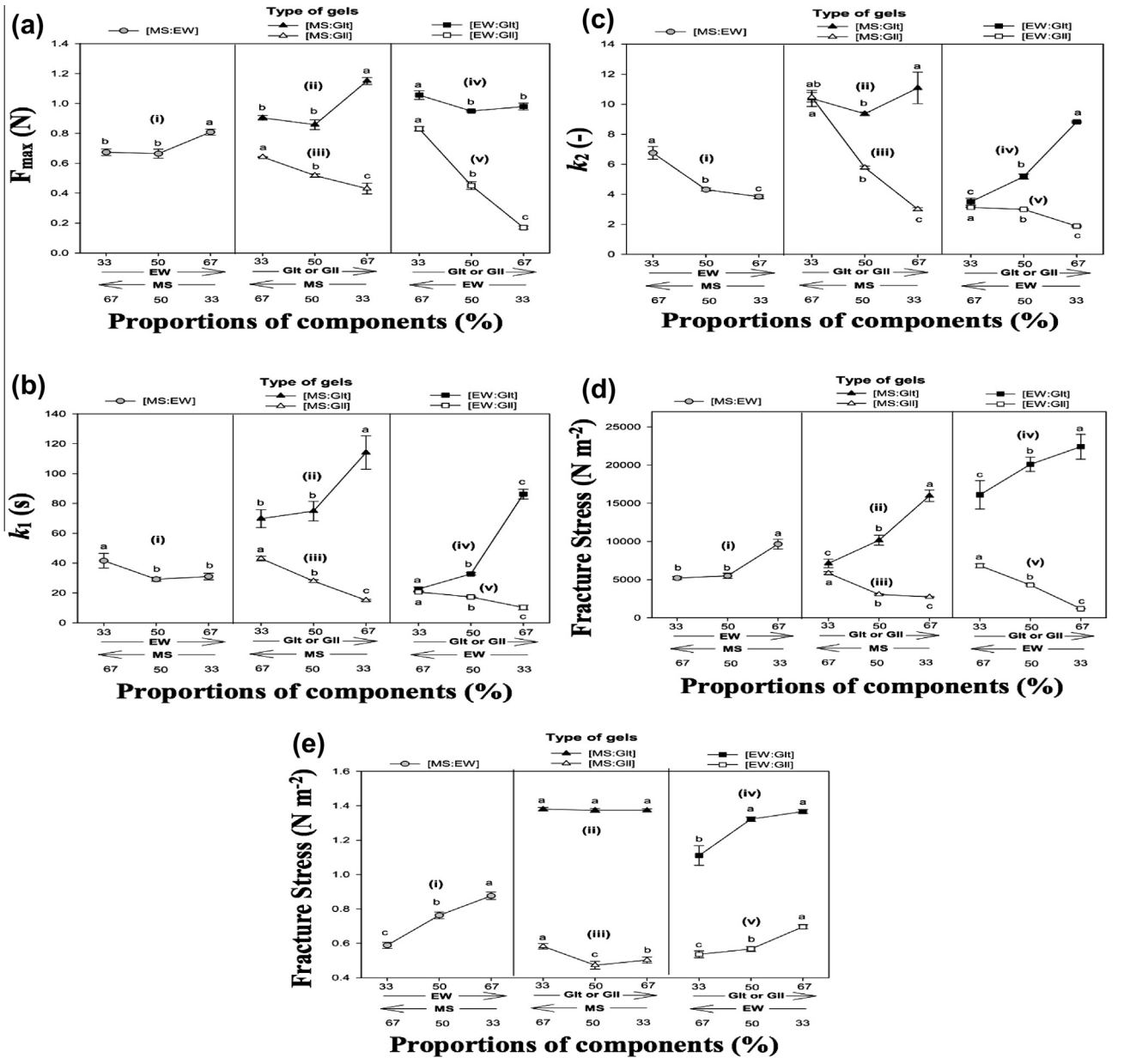

Figure 2 Stress relaxation parameters; (a) F_{max}, (b) k_1 and (c) k_2, and uniaxial compression parameter; (d) fracture stress and (e) fracture strain of BCG: (i) [MS:EW], (ii) [MS:Glt], (iii) [MS:Gll], (iv) [EW:Glt] and (v) [EW:Gll]. Data points are mean ± standard deviation ($n = 5$). Different letters on each symbol indicate significant difference ($P < 0.05$) among samples of different proportions for each type of BCG.

The Gll-TCG with [MS:EW:Gll] ratios of [17:17:67], [17:42:42], [33:33:33] and [42:17:42] showed the lowest levels of F_{max} (Fig. 3a (ii)). This demonstrates that these TCG were very weak and not self-supporting. The behavior tendencies of k_1 and k_2 for Gll-TCG were similar as depicted in Fig. 3b (ii) and c (ii). The network of Gll-TCG became weaker and more brittle with a lower level of solidity as the proportions of Gll increased. The values of k_1 and k_2 increased with the increasing proportions of MS that resulted in the formation of more elastic network strands with a more compact gel structure. However, both the EW and Gll led to the formation of more rigid and brittle network strands. Consequently, the Gll-TCG formed with high proportions of EW or Gll consisted of higher content of viscous components.

3.2. Large deformation – fracture properties

3.2.1. Fracture properties of SCG and BCG

The fracture stress and fracture strain values of SCG and BCG were plotted against each other (Fig. 4a). Glt-SCG fractured at the highest levels of stress and strain indicating the gel was strong and highly elastic. One of the suggested reasons for the high rupture strains for Glt-SCG is the longer, more flexible chains linking adjacent crosslinks in Glt network

(Bot et al., 1996). Gll-SCG was the most fragile and brittle relative to the other gels as indicated by the lowest level of stress and strain. Thus, Gll-SCG ruptured easily into a large amount of small pieces. This was in accordance with the texture profile analysis reported by Foo et al. (2013) for gellan gels. On the other hand, MS-SCG and EW-SCG showed similar fracture stress of ~24,500 N m^{-2}, however, MS-SCG ruptured at a lower strain level indicating that MS-SCG was less deformable relative to EW-SCG. The strong gel network of EW-SCG could be due to stabilization of egg protein by intermolecular linkages (e.g. disulfide cross-link, hydrogen bonds and hydrophobic interaction) during EW gelation (Lee and Chen, 2002; Weijers et al., 2006) as compared to hydrogen bonds and van der Waals forces in MS-SCG (Yoon et al., 2009), in which the former was known to be stronger as compared to the latter (Renkema and van Vliet, 2002).

From the fracture profiles, all the combinations of BCG were relatively weaker as compared to their respective SCG (Fig. 4a). In general, all the BCG consisted of Glt were stronger and relatively more deformable. While, all the Gll-BCG could be categorized as weak and brittle. The [MS:EW]-BCG fell in the intermediate range among Glt-BCG and Gll-BCG. The effect of component proportions on fracture stress and fracture strain of BCG is exhibited in Fig. 2d and e, respectively.

The fracture stress of [MS:EW]-BCG at the ratio of [33:67] was significantly ($P < 0.05$) higher than [MS:EW]-BCG formed at an equal or a lower level of EW, in which these latter exhibited similar fracture stress values (Fig. 2d (i)). On the other hand, the fracture strain values of [MS:EW]-BCG increased significantly ($P < 0.05$) as the EW proportion increased (Fig. 2e (i)). The increase in fracture strain values could be due to the increase in the disulfide bonds in the gel formation since the EW proportion increased (Weijers et al., 2006). This suggests that the proportions of MS and EW greatly affected the types of bonds within the gels.

For [MS:Glt]-BCG, fracture stress increased significantly ($P < 0.05$) with increasing proportions of Glt while fracture strain remained at the similar levels (Fig. 2d (ii) and e (ii)). This implies that the increase of Glt proportions in [MS:Glt]-BCG could improve the gel strength while the type of gel network remained the same.

The increase in Gll proportions significantly ($P < 0.05$) reduced the gel strength of [MS:Gll]-BCG (Fig. 2d (iii)). However, the fracture strain of [MS:Gll]-BCG with equal or lower proportions of Gll was low (Fig. 2e (iii)). This suggests that with the increasing proportions of Gll, [MS:Gll]-BCG became weaker, brittle and prone to rupture.

For [EW:Glt]-BCG, the increasing proportions of Glt resulted in the increase in fracture stress and fracture strain (Fig. 2d (iv) and e (iv)). However, with equal or higher proportions of Glt the fracture strains were not different significantly ($P > 0.05$), suggesting that the increase of Glt resulted in stronger and more elastic [EW:Glt]-BCG.

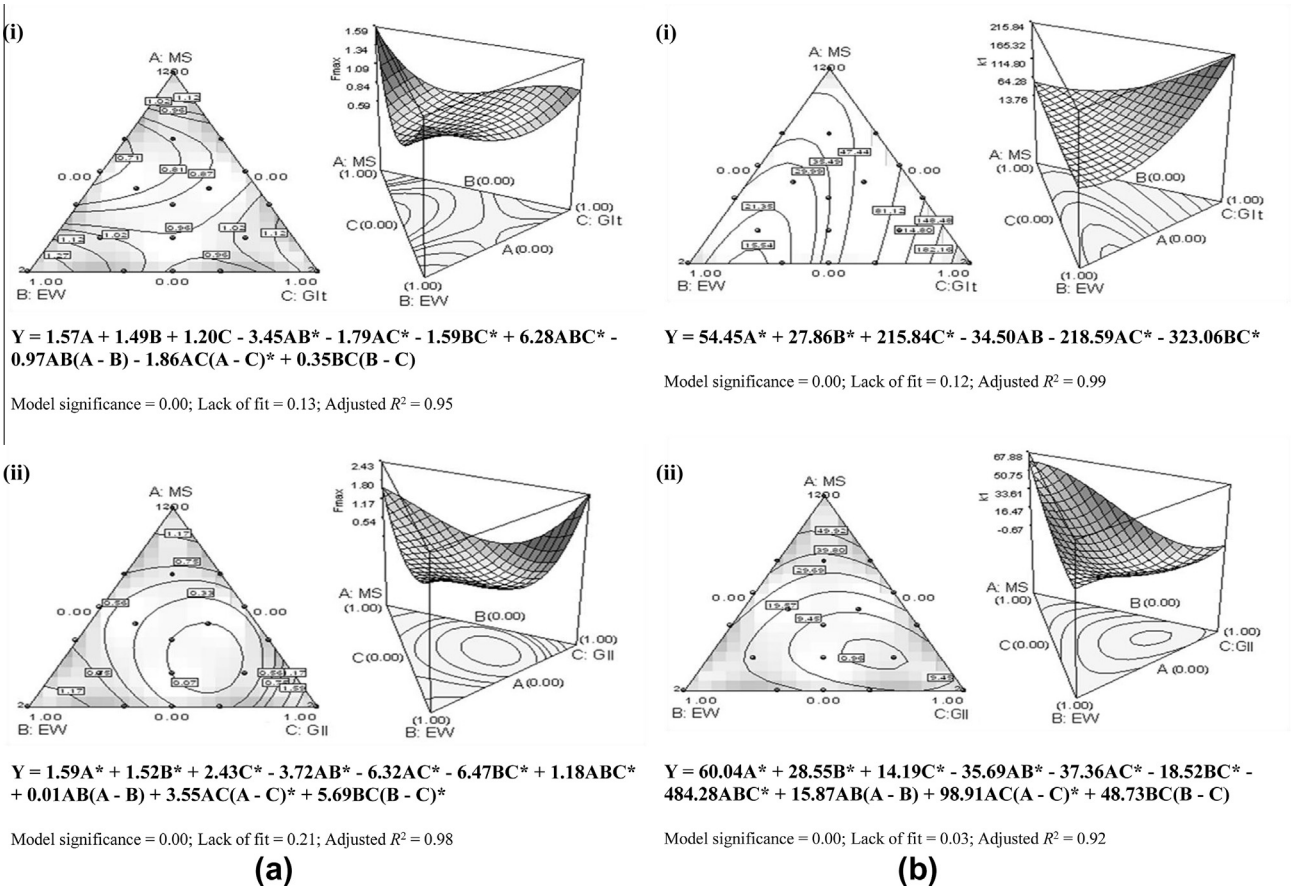

Figure 3 Surface and contour plots of stress relaxation parameter; (a) F_{max}, (b) k_1 and (c) k_2, and uniaxial compression parameter; (d) fracture stress and (e) fracture strain for (i) [MS:EW:Glt]-TCG and (ii) [MS:EW:Gll]-TCG.

(i)

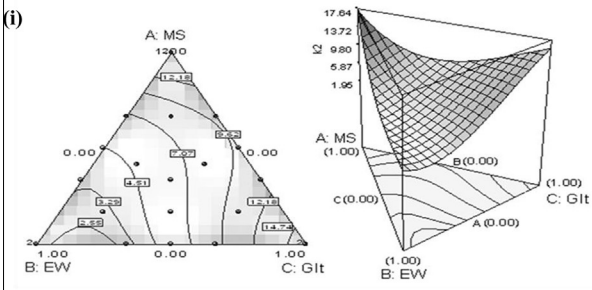

Y = 17.30A* + 3.26B* + 16.00C* - 23.33AB* - 26.88AC* - 16.20BC* + 37.46ABC* - 9.15AB(A - B) - 11.41AC(A - C)* - 12.98BC(B - C)*

Model significance = 0.00; Lack of fit = 0.66; Adjusted R^2 = 0.98

(i)

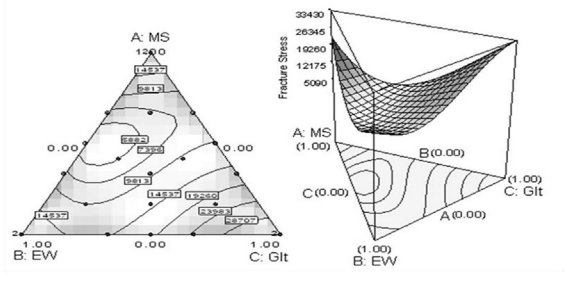

Y = 122774A* + 21690B* + 33430C* - 67376AB* - 71753AC* - 36214BC* + 81402ABC - 8007AB(A - B) - 35018AC(A - C) - 43618BC(B - C)*

Model significance = 0.00*; Lack of fit = 0.08; Adjusted R^2 = 0.95

(ii)

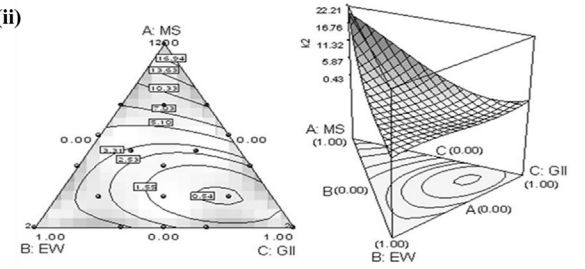

Y = 20.24A* + 3.16B* + 3.01C* - 28.30AB* - 22.69AC* - 1.27BC - 35.77ABC - 16.15AB(A - B)* + 15.85AC(A - C)* + 9.00BC(B - C)

Model significance = 0.00; Lack of fit = 0.00*; Adjusted R^2 = 0.98

(ii)

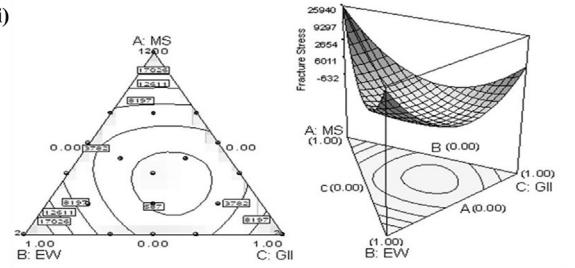

Y = 25855A* + 25200B* + 14788C* - 82517AB* - 70604AC* - 69277BC* - 65226ABC*

Model significance = 0.00*; Lack of fit = 0.05; Adjusted R^2 = 0.98

(c) **(d)**

(i)

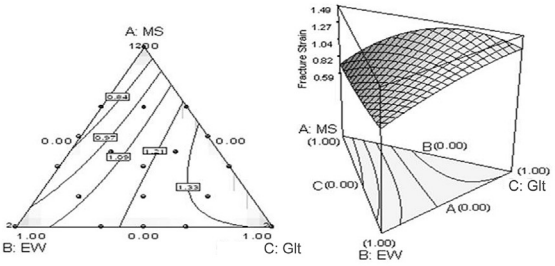

Y = 0.72A* + 1.02B* + 1.33C* - 0.18AB + 1.42AC* + 0.26BC

Model significance = 0.00*; Lack of fit = 0.00*; Adjusted R^2 = 0.66

(ii)

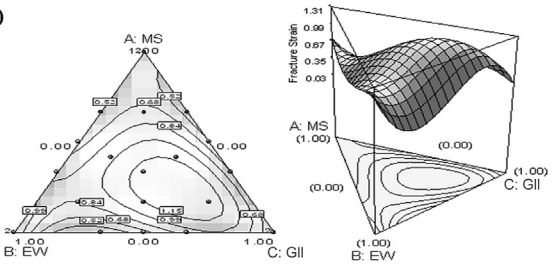

Y = 0.73A* + 1.19B* + 0.48C* - 1.40AB - 0.23AC - 0.89BC + 18.74ABC - 0.75AB(A - B) - 2.37AC(A - C) - 5.18BC(B - C)*

Model significance = 0.01*; Lack of fit = 0.00*; Adjusted R^2 = 0.57

(e)

Fig. 3 (*continued*)

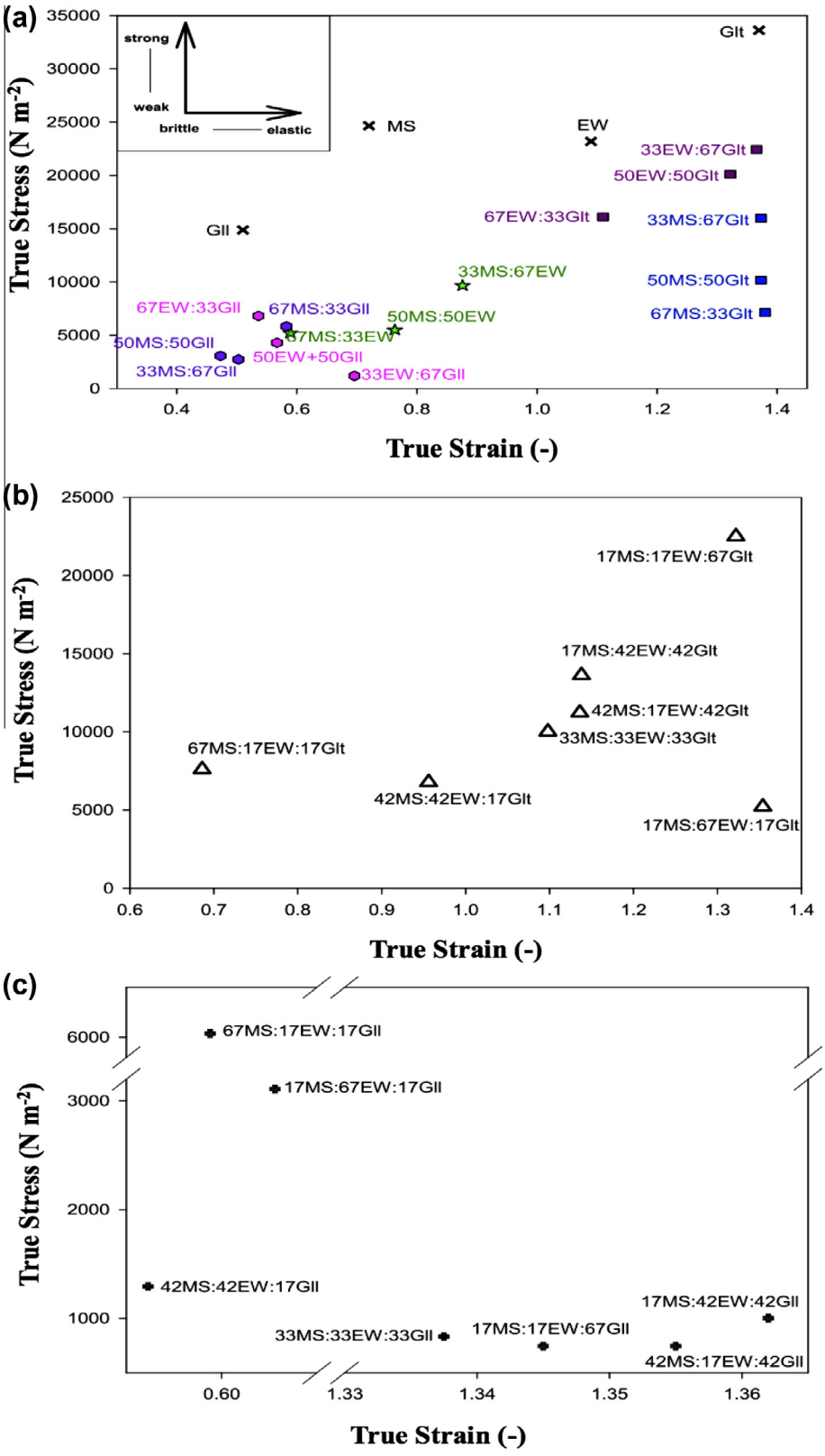

Figure 4 Fracture properties of (a) SCG and BCG, (b) Glt-TCG and (c) Gll-TCG.

The gel strength of [EW:Gll]-BCG increased significantly ($P < 0.05$) with the increase of Gll proportions (Fig. 2d (v)). On the contrary, the reverse trend was observed for fracture strain where [EW:Gll]-BCG became significantly ($P < 0.05$) less deformable with higher proportions of Gll (Fig. 2e (v)).

3.2.2. Fracture properties of TCG

Fracture properties of Glt-TCG and Gll-TCG are described in Fig. 4b and c, respectively. The effects of proportional changes on fracture stress and fracture strain of Glt-TCG and Gll-TCG could be observed from the patterns of the respective contour and surface plots as shown in Fig. 3d and e.

Glt-TCG with the lowest proportions of Glt displayed fracture stress less than 10,000 N m^{-2}, while these TCG became more deformable with increasing EW proportions (Fig. 4b). For Glt-TCG, Glt was the dominant component contributed to the strength and elasticity of the gel network as represented by the fracture stress and fracture strain (Fig. 3d (i) and e (i)). At the low proportions of Glt, the equal proportions of MS and EW yielded TCG with the lowest fracture stress but did not affect the fracture strains. This suggests that at low proportions of Glt, similar types of networks were formed within Glt-TCG.

Gll-TCG with low levels of fracture stress (< 1000 N m^{-2}) and high levels of strains (> 1.33) were not self-standing (Fig. 4c). Only Gll-TCG gels formed with the least proportions (17%) of Gll were stronger and more brittle as compared to the rest of Gll-TCG blends. From the contour and surface plots of fracture stress for Gll-TCG, the mixture of three components induced antagonistic effect on the gel strength (Fig. 3d (ii)). Gll-TCG yielded with equal proportions displayed the highest level of fracture strains (Fig. 3e (ii)). However, these Gll-TCG were not elastic but became ductile and the Gll-TCG did not rupture but flowed at low levels of stress.

4. Conclusion

Glt and Gll composite gels with MS or/and EW were evaluated by small (stress relaxation) and large deformation (fracture properties) tests. Glt composite gels were relatively stronger and more elastic as the network strands were more flexible and the gel structure became more compact. On the contrary, Gll resulted in more rigid and brittle network strands in Gll composite gels with less compact structure. Thus, the Gll composite gels were weaker, possessed more viscous behavior. Although Gll composite gels showed high levels of strain, these gels were not elastic but became ductile as the gels did not fracture and flowed under at low stress levels. In conclusion, Glt and Gll exerted different effects on rheological properties in either binary or ternary composite gel systems. The data obtained from the present study could provide valuable information to proceed with further investigation on the fundamental as well as the application prospect. It would be interesting to further explore the microstructure and breakdown behavior of Glt and Gll composite gels from the sensory aspect.

Acknowledgements

This project was supported by the Fundamental Research Grant Scheme (Grant No. 203/PTEKIND/671199) from the Ministry of Higher Education Malaysia. The fellowship for Dr. Foo Wan Teck and Dr. Tan Thuan Chew provided by USM is gratefully acknowledged. In addition, we gratefully acknowledge and are indebted to the anonymous referees for comments and constructive suggestions provided for improving the manuscript.

References

Bot, A., van Amerongen, I.A., Groat, R.D., Hoekstra, N.L., Agterof, W.G.M., 1996. Large deformation rheology of gelatin gels. Polym. Gels Networks 4, 189–227.

Burey, P., Bhandari, B.R., Rutgers, R.P.G., Halley, P.J., Torley, P.J., 2009. Confectionery gels: a review on formulation, rheological and structural aspects. Int. J. Food Prop. 12, 176–210.

Foo, W.-T., Liong, M.-T., Easa, A.M., 2013. Textural and structural breakdown properties of selected hydrocolloid gels. Food Res. Int. 52, 401–408.

Glicksman, M., 1969. Starches. In: Glicksman, M. (Ed.), Gum Technology in the Food Industry. Academic Press, New York.

Hibberd, G.E., Wallace, W.J., 1966. Dynamic viscoelastic behaviour of wheat flour doughs. Rheol. Acta 5, 193–198.

Hongsprabhas, P., 2011. Viscoelastic properties of mixed flour gels. Sci. Asia 27, 169–175.

Houzè, G., Cases, E., Colas, B., Cayot, P., 2005. Viscoelastic properties of acid milk gel as affected by fat nature at low level. Int. Dairy J. 15, 1006–1016.

Huang, M., Kennedy, J.F., Li, B., Xu, X., Xie, B.J., 2007. Characters of rice starch gel modified by gellan, carrageenan, and glucomannan: a texture profile analysis study. Carbohydr. Polym. 69, 411–418.

Ibrahim, N.H., Man, Y.B.C., Tan, C.P., Idris, N.A., 2010. Mixture design experiment on flow behaviour of O/W emulsions as affected by polysaccharide interactions. World Acad. Sci. Eng. Technol. 67, 1000–1006.

Jaya, S., Durance, T.D., 2008. Stress relaxation behavior of microwave-vacuum-dried alginate gels. J. Texture Stud. 39, 183–197.

Joshi, M., Aldred, P., Panozzo, J.F., Kasapis, S., Adhikari, B., 2014. Rheological and microstructural characteristics of lentil starch-lentil protein composite pastes and gels. Food Hydrocolloid. 35, 226–237.

Kampf, N., Nussinovitch, A., 1997. Rheological characterization of κ-carrageenan soy milk gels. Food Hydrocolloid. 11, 261–269.

Ledward, D.A., 2000. Gelatin. In: Williams, P.A., Philips, G.O. (Eds.), Handbook of Hydrocolloids. CRC Press, Boca Raton.

Lee, W.C., Chen, T.C., 2002. Functional characteristics of egg white solids obtained from papain treated albumen. J. Food Eng. 51, 263–266.

Lee, K.Y., Shim, J., Bae, I.Y., Cha, J., Park, C.S., Lee, H.G., 2003. Characterization of gellan/gelatin mixed solutions and gels. Lebensm. Wiss. Technol. 36, 795–802.

Luyten, H., van Vliet, T., 1995. Fracture properties of starch gels and their rate dependency. J. Texture Stud. 26, 281–298.

Mao, R., Tang, J., 1999. Texture properties of gellan gels as affected by temperature. J. Texture Stud. 30, 409–433.

Morris, E.R., Nishinari, K., Rinaudo, M., 2012. Gelation of gellan – a review. Food Hydrocolloid. 28, 373–411.

Morrison, N.A., Sworn, G., Clark, R.C., Chen, Y.L., Talashek, T., 1999. Gelatin alternatives for the food industry. Prog. Coll. Pol. Sci. 114, 127–131.

Panouillé, M., Larreta-Garde, V., 2009. Gelation behaviour of gelatin and alginate mixtures. Food Hydrocolloid. 23, 1074–1080.

Peleg, M., Normand, M.D., 1983. Comparison of two methods for stress relaxation data presentation of solid foods. Rheol. Acta. 22, 108–113.

Pérez-Campos, S.J., Chavarría-Hernández, N., Tecante, A., Ramírez-Gilly, M., Rodríguez-Hernández, A.I., 2012. Gelation and microstructure of dilute gellan solutions with calcium ions. Food Hydrocolloid. 28, 291–300.

Renkema, J.M.S., 2004. Relations between rheological properties and network structure of soy protein gels. Food Hydrocolloid. 18, 39–47.

Renkema, J.M.S., van Vliet, T., 2002. Heat-induced gel formation by soy proteins at neutral pH. J. Agric. Food Chem. 50, 1569–1573.

Shim, J., Mulvaney, S.J., 2001. Effect of heating temperature, pH, concentration and starch/whey protein ratio on the viscoelastic properties of corn starch/whey protein mixed gels. J. Sci. Food Agric. 81, 706–717.

Singh, H., Rockall, A., Martin, C.R., Chung, O.K., Lookhart, G.L., 2006. The analysis of stress relaxation data of some viscoelastic foods using a texture analyzer. J. Texture Stud. 37, 383–392.

Tang, J., Tung, M.A., Zeng, Y., 1998. Characterization of gellan gels using stress relaxation. J. Food Eng. 38, 279–295.

van Vliet, T., 1996. Large deformation and fracture behaviour of gels. Curr. Opin. Colloid Interface Sci. 1, 740–745.

Weijers, M., van de Velde, F., Stijnman, A., van de Pijpekamp, A., Visschers, R.W., 2006. Structure and rheological properties of acid-induced egg white protein gels. Food Hydrocolloid. 20, 146–159.

Williams, P.A., Philips, G.O., 2003. The use of hydocolloids to improve food texture. In: McKenna, B.M. (Ed.), Texture in Food, Semi-solid Foods, vol. 1. Woodhead Publishing Limited, Cambridge.

Wium, H., Qvist, K.B., 1997. Rheological properties of UF-FETA cheese determined by uniaxial compression and dynamic testing. J. Texture Stud. 28, 435–454.

Yoon, H.-S., Lee, J.H., Lim, S.-T., 2009. Utilization of retrograded wazy maize starch gels as tablet matrix for controlled release of theophylline. Carbohydr. Polym. 76, 449–453.

Zhang, J., 2004. Mechanisms responsible for non-linear and fracture properties of gel-based foods, Doctor of Philosophy dissertation. North Carolina State University, Raleigh.